

Response to Review of “Description and basic evaluation of BNU-ESM version 1” by D. Ji et al.

We first thank the reviewer for his/her constructive comments, which helped us clarify and greatly improve the paper. Comments from the reviewer are in black, and our responses are in blue.

Major Comments:

This study evaluates the coupled model performance of BNU-ESM. The authors described several important aspects of model simulated fields. However, a systematic way to evaluate the model may be necessary. For example, a standard set of metrics and diagnostics for climate model performance evaluation is needed (see comments below). Also, the authors mention the carbon-climate feedbacks. Yet, the evaluations of global carbon cycle or land model performance are not included in the present manuscript.

Another important aspect is the future development plan of the model which is barely mentioned. I suggest the authors can spend one section to address the model development plan on (1) near term focus of model parameterizations improvement, (2) vertical and horizontal resolutions of model components, (3) development or improvement of dynamical core of atmospheric or oceanic models. For example, most of the parameterizations in the atmospheric model, such cloud macro-, micro-physics had changed significantly from CAM3.5 to CAM5. Some well know model biases such as clouds have been improved from CAM3.5 to CAM5. How to address this issue in the BNU-ESM is important for these paper. Based on these and comments below, I recommend major revision for the current manuscript.

Agree and thanks for these insightful comments. Performance evaluation for BNU-ESM with a standard set of metrics and diagnostics is answered below in specific comment 2. A section on describing terrestrial land carbon cycle and a section on the future development plan will be added in the final revised paper based on the following text:

Terrestrial primary production

Carbon flux components are hard to measure directly, presenting a challenge in evaluating the model performance. Global products for land gross primary production (GPP) and net primary production (NPP) exist but are model-based and have large uncertainties (Anav et al., 2013; Ito, 2011). Figure R1 shows regional averages of monthly land gross primary production (GPP) for BNU-ESM compared with FLUXNET-MTE estimates (Jung et al., 2011). BNU-ESM replicates the annual cycle of GPP in arctic, mid-latitudes, and tropical regions, but the model has a tendency for underestimation during boreal summer, especially over Alaska, the eastern USA, and Europe. Differences between the estimates from our model and those from FLUXNET-MTE may be caused both by differences in the near surface climatology and land cover characteristics, as BNU-ESM dynamically simulates vegetation characteristics as a function of climate and atmospheric CO₂ concentration. In Alaska, the model simulates more C₃ arctic grass and less boreal shrub compared with the observed IGBP vegetation distribution (not shown). While in the Europe, although the model simulates more broadleaf deciduous temperate tree cover and less grassland, the biased high temperature and low precipitation during boreal summer suppress GPP significantly. In the Amazon, the model simulates a reasonable vegetation distribution of broadleaf and evergreen tropical trees, but the wet season precipitation suffers a dry bias until August (Fig. 2), and the model systematically underestimates GPP. The interannual variability of the GPP estimated by the model is larger than the observational estimates from FLUXNET-MTE and this may be connected with the stronger interannual variability of the physical fields.

The global terrestrial GPP simulated in the BNU-ESM is 106.3 Pg C yr⁻¹ over the period 1986-2005. Various studies estimated the global terrestrial GPP to be about 120 ± 6 Pg C yr⁻¹ over similar periods (Sabine et al. 2004; Beer et al. 2010; Jung et al. 2011). However, these are well below the range of 150-175 Pg C yr⁻¹ from recent observational estimates (Welp et al., 2011). The global simulated NPP over the period 1986-2005 is 49 Pg C yr⁻¹, which is consistent with the range of 42-70 Pg C yr⁻¹ from earlier studies (Schimel et al., 2001; Gruber et al., 2004; Zhao et al., 2005; Ito, 2011). Net biosphere production (NBP) simulated in the model for the 1990s and 2000-2005 are 1.6 Pg C yr⁻¹ and 1.4 Pg C yr⁻¹, which is also consistent with estimates of 1.5 ± 0.8 Pg C yr⁻¹ and 1.1 ± 0.8 Pg C yr⁻¹

respectively reported by Ciais et al. (2013).

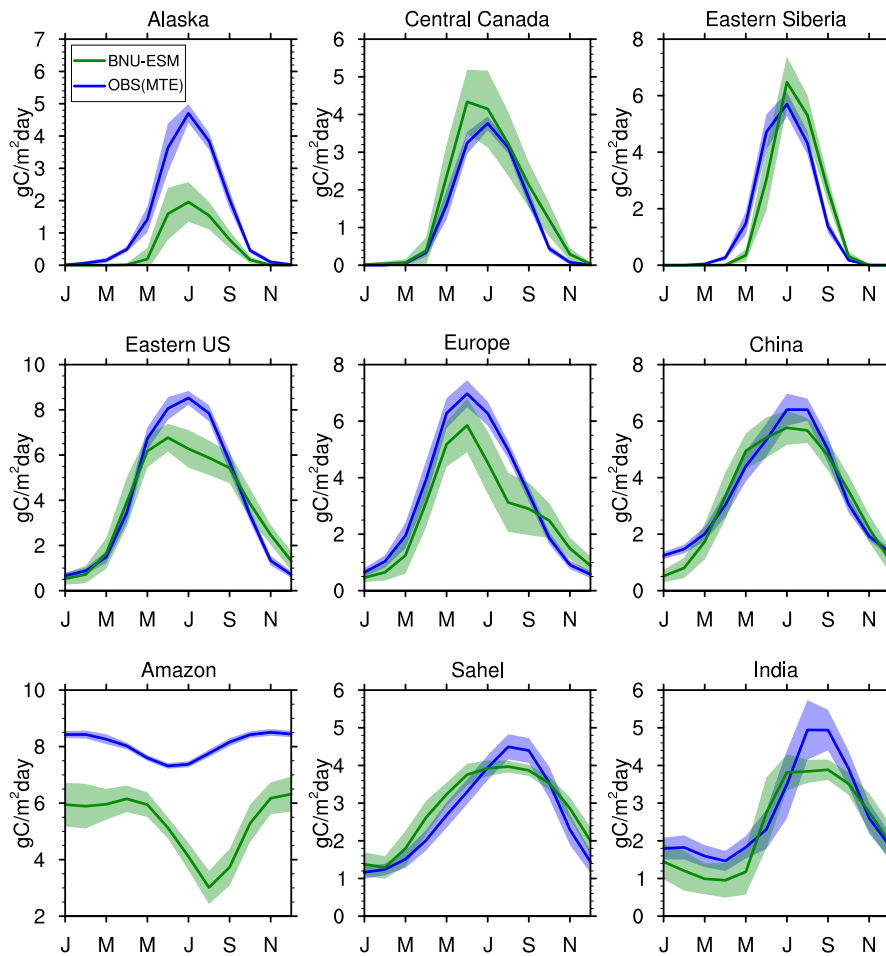


Figure R1. As for Fig. 1, but for GPP for the period 1986–2005. The observations (MTE) are from FLUXNET-MTE estimates (Jung et al., 2011).

Soil organic carbon

Soil organic carbon is a large component of the carbon cycle that can participate in climate change feedbacks, particularly on decadal and centennial timescales (Todd-Brown et al., 2013). The amount of soil organic carbon simulated by models is strongly dependent on their design, especially the number of soil carbon pools, turnover rate of decomposition and their response to soil moisture and temperature change. Figure R2a, R2b show the distribution of global soil organic carbon content, including litter, from BNU-ESM compared with the most recent high-resolution observation-based

Harmonized World Soil Database (HWSD; FAO/IIASA/ISRIC/ISSCAS/JRC, 2012). The HWSD data provides soil carbon estimates for topsoil (0-30 cm) and subsoil (30-100 cm) at 30-arc-second resolution. Overall, the ecosystem carbon content follows the precipitation and temperature distribution (Fig. 3 and Fig. 4). The BNU-ESM model can capture the large store of soil organic carbon in the boreal and tundra regions of Eurasia and North America, and the small storage in tropical and extra-tropical regions (Fig. R2b). The model underestimates soil carbon density in the upper 1 m globally compared with the HWSD (Fig. R2a), especially in boreal regions. Soil carbon is overestimated in the model on the Tibetan plateau, because the coarse horizontal resolution does not correctly represent the rugged terrain and overestimates vegetation cover.

The total simulated soil organic carbon, including litter, is 700 Pg C for the period 1986-2005, is well below the 1260 Pg C (with a 95% confidence interval of 890-1660 Pg C) estimated from HWSD data (Todd-Brown et al., 2013), and 1502 Pg C estimated by Jobbágy and Jackson (2000) for the upper 1 m of soil. However, there is still considerable uncertainty for those observation-based estimates because of limited numbers of soil profiles with organic carbon analyses (Tarnocai et al., 2009). In addition, the soil carbon sub-model of BNU-ESM is not yet designed to simulate the large carbon accumulations in organic peat soils, or the stocks and dynamics of organic matter in permafrost, a common failure of many CMIP5 models. It is thus to be expected that simulations without these processes underestimate the global soil organic carbon stock. Especially, the temperature sensitivity of soil carbon decomposition is described by the Q_{10} equation (Lloyd and Taylor, 1994) in BNU-ESM, and the environmental controls of moisture and temperature are diagnosed at 0.25 m depth. In Figure R2c, the zonally averaged soil carbon density from BNU-ESM is compared with those from HWSD and IGBP-DIS for upper 0.3 m and upper 1.0 m depth ranges. The model simulates substantially less soil carbon than those from the HWSD and IGBP-DIS for the upper 1.0 m, but agrees much better with upper 0.3 m soil carbon density estimates on magnitude and latitudinal gradients.

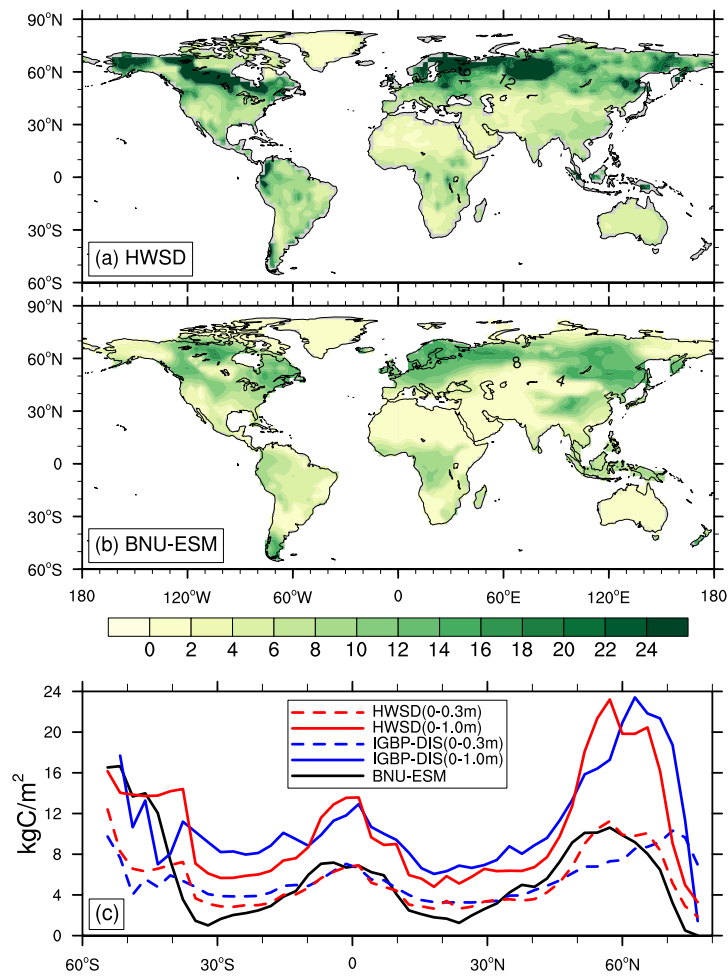


Figure R2. Soil carbon density in the top 1 m depth from the HSWD (a) and BNU-ESM (b), and zonal average soil carbon density of BNU-ESM compared with that of upper 0.3 m and upper 1 m soil from HSWD, IGBP-DIS data sets.

Future model development plan

Currently BNU-ESM is evolving in many respects. As global biogeochemical cycles are recognized as being evermore significant in mediating global climate change, improvements of BNU-ESM are underway in the terrestrial and marine biogeochemistry schemes. On terrestrial biogeochemistry, the LPJ-DyN based carbon-nitrogen interaction scheme (Xu and Prentice, 2008) will be evaluated and activated in future. A dynamic marine ecosystem scheme will replace the current iBGC module, the new marine ecosystem scheme has improved parameterizations of dissolved organic materials and detritus (Wang et al., 2008), a phytoplankton dynamic module that produces a variable

of carbon to chlorophyll ratio (Wang et al., 2009a), and refined nitrogen regeneration pathways (Wang et al., 2009b). Additionally, a three-dimensional canopy radiative transfer model (Yuan et al., 2014) will replace the traditional one-dimensional two-stream approximation scheme in the land component to calculate more realistic terrestrial canopy radiation. The spatial resolution of the BNU-ESM will be increased to better simulate more realistic surface physical climate, especially for the atmospheric and land components. Currently a $0.9^\circ \times 1.25^\circ$ resolution land and atmosphere components adapted from the finite-volume dynamic core in CAM is being tested. We also note that CAM5 has made significant progress, such as correcting well know cloud biases from CAM3.5 (Kay et al., 2012). Discussion of how to incorporate these developments from CAM5 into BNU-ESM is underway.

Specific comments:

1. A figure showing the time series of global net energy budget at TOA and surface are necessary to indicate whether the model is in energy balance or not. Also, another figure of time series of global mean sea surface temperature to indicate the climate drift would be necessary.

Agree and Done.

Global mean TOA net radiation flux over *piControl* period is 0.88 W/m^2 , while global mean surface net radiation flux is 0.86 W/m^2 . The global mean sea surface temperature over *piControl* period is $17.69 \text{ }^\circ\text{C}$, and has a warming drift of $0.02 \text{ }^\circ\text{C}$ per century.

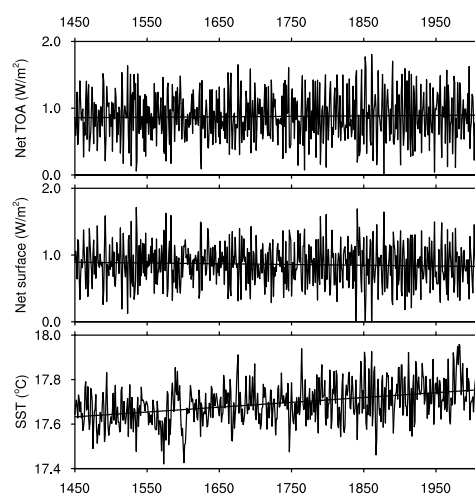


Figure R3. The global mean TOA and surface net radiation flux, global mean SST over the

piControl simulation period. The black lines are linear regressions.

2. Standard metrics of several simulated global fields on a Taylor diagram to summarize model performance is recommend as shown in Fig.1 of Gleckler et al. (2008), Journal of Geophysical Research, Atmospheres.

Agree and thanks for this constructive suggestion. The following model performance summary based on Taylor diagram will be included in the final revised paper.

To systematically evaluate the general performance of BNU-ESM, we use the Taylor diagram (Taylor, 2001; Gleckler et al., 2008), which relates the “centered” root-mean square (RMS) error, the pattern correlation and the standard deviation of particular climate fields. We selected 24 fields (Table 1) and compared model simulations with two different reference data sets (only one dataset was available for gross primary production over land and surface CO₂ flux over ocean). The selection rationale for the fields and reference data sets follows Gleckler et al. (2008), where most of reference data sets are briefly described. One notable difference is that we use ERA-Interim (Dee et al., 2011) and JRA-55 (Ebita et al., 2011) reanalysis data instead of ERA40 and NCEP to reflect recent advances in reanalysis systems. We use estimates of specific humidity from National Aeronautics and Space Administration (NASA) Modern Era Retrospective analysis for Research and Applications (MERRA, Rienecker et al., 2011) instead of the Atmospheric Infrared Sounder (AIRS) experiment, as Tian et al. (2013) indicated MERRA specific humidity probably has a smaller uncertainty than the AIRS data set. The International Satellite Cloud Climatology Project (ISCCP, Rossow and Schiffer, 1999; Rossow and Dueñas, 2004) D2 and CLOUDSAT (L'Ecuyer et al., 2008) data sets are used to examine the total cloud cover. The Clouds and the Earth's Radiant Energy System - Energy Balanced and Filled (CERES-EBAF) data set (Loeb et al., 2009) is used instead of the CERES observations, because the energy balanced characteristics of CERES-EBAF that made it more suitable for the near balanced energetics of the earth system. Two carbon cycle fields (gpp and fgco2) were added to fill the gap between climate system model and earth system model. The reference data used to examine gross primary production (gpp) over land is FLUXNET Model Tree Ensembles (FLUXNET-MTE) estimates (Jung et al., 2011), which are restricted to vegetated land surface. The reference

data used to examine surface CO₂ flux over ocean (fgco2) is from Lamont-Doherty Earth Observatory (LDEO, Takahashi et al., 2009), this climatology data set was created from about 3 million direct observations of seawater pCO₂ around the world between 1970 and 2007.

Figure R4 shows six climatological annual-cycle space-time Taylor diagrams for the 24 selected fields in Table 1 for the tropical (20S-20N) and the northern extra-tropical (20N-90N) zones. It is clear from Figure R4 that the accuracy of the model varies between fields and domains. Some simulated fields over the northern extra-tropics have correlations with the reference data of greater than 0.95 (e.g., zg-500hPa, ta-850hPa, rlut, rsnt, tos), and most of fields have correlations with the reference data of greater than 0.8, whereas one field has much lower correlation of 0.38 (fgco2 over the northern extra-tropics). The amplitude of spatial and temporal variability simulated by the model is reasonably close to that observationally based reference data. The normalized standard deviations between the simulation and the reference data of most fields have a bias of less than 0.25, and several fields have a bias of less than 0.1 (e.g., ta-850hPa, hus-850hPa, rlut, rsnt, psl, tos). One outlier in Fig. R4 (NHEX G3 and TROP G3) is the sensible heat flux over ocean (hfss) examined with NOCS reference data [Josey et al., 1999]. The model shows better skills when compared to ERA-Interim reanalysis, although the pattern correlations against two reference data sets are both of about 0.6. Previous studies suggest that there are large uncertainties in NOCS data set, and their pattern has better agreement with reanalysis products than the magnitude of their fluxes (e.g., Taylor, 2000). In general, most of fields over the tropics are closer to reference data than those over the northern extra-tropics in Taylor diagrams, but some fields with relatively high correlations in the northern extra-tropics have a lower skill in the tropics. These features are consistent with Gleckler et al. (2008).

Table 1. Observationally Based Reference Data Sets

Variable I.D.	Description	Reference1/Reference2	Domain
ta	Temperature [°C]	¹ ERA-Interim/ ² JRA-55	200, 850 hPa
ua	Zonal wind [m s ⁻¹]	¹ ERA-Interim/ ² JRA-55	200, 850 hPa
va	Meridional wind [m s ⁻¹]	¹ ERA-Interim/ ² JRA-55	200, 850 hPa

zg	Geopotential height [m]	¹ ERA-Interim/ ² JRA-55	500 hPa
hus	Specific humidity [kg kg ⁻¹]	¹ ERA-Interim/ ³ MERRA	400, 850 hPa
rlut	TOA outgoing longwave radiation [W m ⁻²]	⁴ ERBE/ ⁵ CERES-EBAF	
rsnt	TOA net shortwave radiation [W m ⁻²]	⁴ ERBE/ ⁵ CERES-EBAF	
rlwcrf	Longwave cloud radiative forcing [W m ⁻²]	⁴ ERBE/ ⁵ CERES-EBAF	Equatorward of 60°
rswcrf	Shortwave cloud radiative forcing [W m ⁻²]	⁴ ERBE/ ⁵ CERES-EBAF	Equatorward of 60°
pr	Total precipitation [mm day ⁻¹]	⁶ GPCP/ ⁷ CMAP	
clt	Total cloud cover [%]	⁸ ISCCP-D2/ ⁹ CLOUDSAT	
prw	Precipitable water [g kg ⁻¹]	¹⁰ RSS(v7)/ ¹¹ NVAP	
psl	Sea level pressure [Pa]	¹ ERA-Interim/ ² JRA-55	Ocean only
uas	Surface (10m) zonal wind speed [m s ⁻¹]	¹ ERA-Interim/ ² JRA-55	Ocean only
vas	Surface (10m) meridional wind speed [m s ⁻¹]	¹ ERA-Interim/ ² JRA-55	Ocean only
tos	Sea surface temperature [°C]	¹² HadISST/ ¹³ OISST(v2)	Ocean only, equatorward of 50°
tauu	Ocean surface zonal wind stress [Pa]	¹ ERA-Interim/ ¹⁴ NOCS	Ocean only
tauv	Ocean surface meridional wind stress [Pa]	¹ ERA-Interim/ ¹⁴ NOCS	Ocean only
hfls(ocn)	Ocean surface latent heat flux [W m ⁻²]	¹ ERA-Interim/ ¹⁴ NOCS	Ocean only
hfss(ocn)	Ocean surface sensible heat flux [W m ⁻²]	¹ ERA-Interim/ ¹⁴ NOCS	Ocean only
hfls(lnd)	Land surface latent heat flux [W m ⁻²]	¹ ERA-Interim/ ¹⁵ FLUXNET-MTE	Land only
hfss(lnd)	Land surface sensible heat flux [W m ⁻²]	¹ ERA-Interim/ ¹⁵ FLUXNET-MTE	Land only
gpp	Gross primary productivity [kg m ⁻² s ⁻¹]	¹⁵ FLUXNET-MTE	Land only
fgco2	Surface CO ₂ flux [kg m ⁻² s ⁻¹]	¹⁶ LDEO	Ocean only

¹ERA-Interim (Dee et al., 2011); ²JRA-55 (Ebita et al., 2011); ³MERRA (Rienecker et al., 2011); ⁴ERBE (Barkstrom, 1984); ⁵CERES-EBAF (Loeb et al., 2009); ⁶GPCP (Adler et al., 2003); ⁷CMAP (Huffman et al., 1997); ⁸ISCCP-D2 (Rossow and Schiffer, 1999; Rossow and Dueñas, 2004); ⁹CLOUDSAT (L'Ecuyer et al., 2008); ¹⁰RSS (Wentz, 2000, 2013); ¹¹NVAP (Simpson et al., 2001); ¹²HadISST (Rayner et al., 2003); ¹³OISST (Reynolds et al., 2002); ¹⁴NOCS (Josey et al., 1999); ¹⁵FLUXNET-MTE (Jung et al., 2011); ¹⁶LDEO (Takahashi et al., 2009);

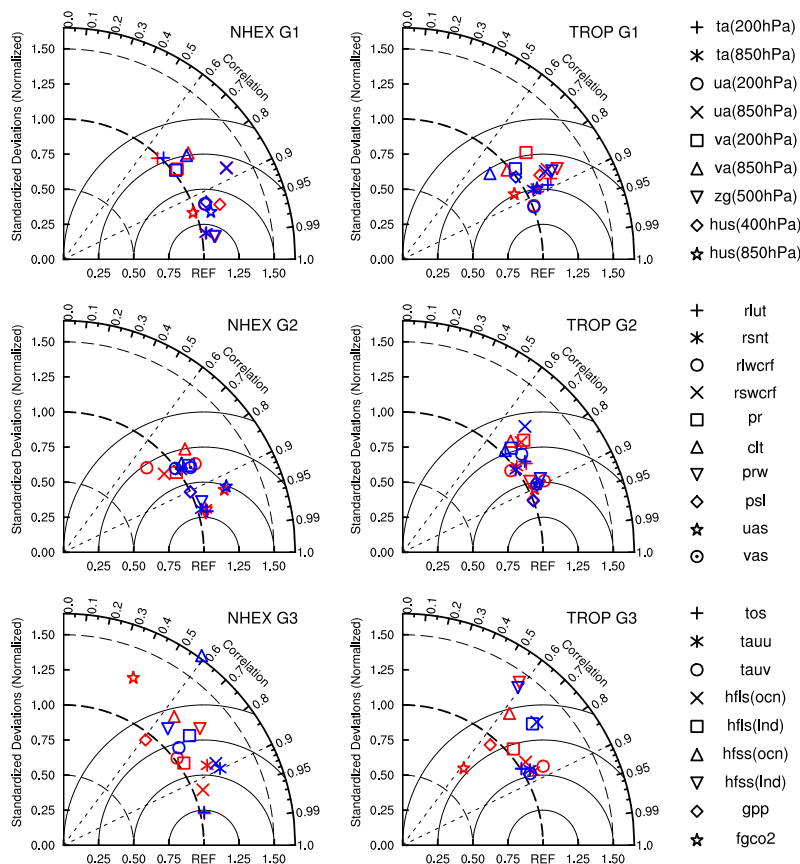


Figure R4. Multivariate Taylor diagrams of the 20th century annual cycle climatological (1986-2005) for the tropical (20S-20N, TROP) and the northern extra-tropical (20N-90N, NHEx) zones. Each field is normalized by the corresponding standard deviation of the reference data, which allows multiple fields to be shown in each sub-figure. Red/Blue markers represent the simulation field evaluated against the Reference1/Reference2 data defined in Table 1.

3. A few sentences to describe the reason why only focus Tropical Pacific SST is necessary.

Agree. We will add the following sentence:

“The tropical Pacific SST is closely associated with the El Niño–Southern Oscillation (ENSO), and exerts a strong influence on the East Asian monsoon (Change et al., 2000; Li et al., 2010).”

4. A power spectrum of the tropical precipitation is recommended.

Agree and Done. The following paragraph and figure will be included in the Tropical Intraseasonal Oscillation section in the final revised paper.

We compared space-time spectra of daily tropical precipitation from BNU-ESM with observed precipitation estimates from GPCP 1 degree daily data set (Huffman et al. 2001) from 1997 to 2005 using the methodology of Wheeler and Kiladis (1999). Figure R5 shows the results of dividing the symmetric raw spectra by estimates of their background spectra. Kelvin, equatorial Rossby (ER), westward inertia-gravity (WIG) waves and the MJO are readily identified in the observational GPCP symmetric spectra. Signals of convectively coupled Kelvin and ER waves appear in the model, and the spectral signature of the MJO is also represented. In observations there is a clear distinction between eastward power in the MJO range (20day-80day) and westward power associated with ER waves. The BNU-ESM model exhibits this distinction to some extent, with the eastward power lying at a constant frequency across all wavenumbers and the westward power lying more along the ER dispersion curves. BNU-ESM represents signals of convectively coupled equatorial waves (CCEWs) similarly as CCSM4 (Hung et al., 2013), such as the equivalent depth of the waves and the low power of WIG waves (Hung et al., 2013, Fig. 4). The powers of eastward propagating components near the MJO spatial and temporal scale in BNU-ESM are more distinctive than that of their westward propagating counterparts compared with CCSM4 (Hung et al., 2013).

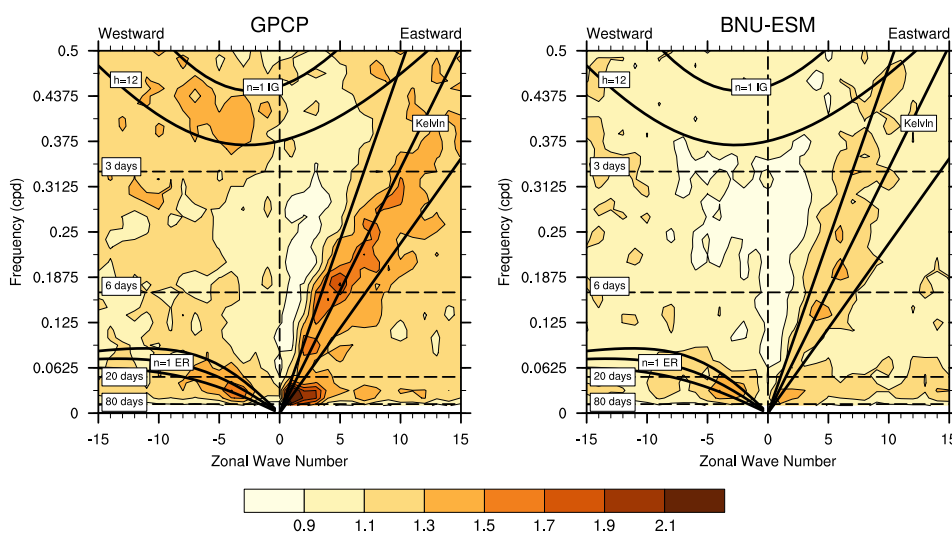


Figure R5. Space-time spectrum of the 15°N–15°S symmetric component of precipitation divided by the background spectrum. Superimposed are the dispersion curves of the odd meridional mode numbered equatorial waves for 12, 25, and 50 m equivalent depths. Frequency spectral width is 1/128 cpd.

Minor Comments:

1. Page 1607, line 3-5: It's not clear which version of the CAM was initially used for the atmospheric model (3.5?). Was it CAM3.5 used and then the convective scheme, chemistry component, and dynamical core were changed from the truck version the CAM. The authors should indicate them clearly.

Agree. To indicate it clearly, we revise line 3-5 to following:

“The atmospheric component in BNU-ESM is based on Community Atmospheric Model version 3.5 (CAM3.5), which is an interim version of the Community Atmospheric Model version 4 (CAM4) (Neale et al., 2010, 2013). Here, the main difference of the atmospheric component in BNU-ESM relative to the original CAM3.5 model is the process of deep convection.”

Also, we revised line 12-18 in Page 1607 to following to state the original schemes being used:

“BNU-ESM uses the Eulerian dynamical core in CAM3.5 for transport calculations with a T42 horizontal spectral resolution (approximately $2.81^\circ \times 2.81^\circ$ transform grid), with 26 levels in the vertical of a hybrid sigma-pressure coordinates and model top at 2.917 hPa. Atmospheric chemical processes utilize the tropospheric MOZART (TROP-MOZART) framework in CAM3.5 (Lamarque et al., 2010), which has prognostic greenhouse gases and prescribed aerosols.”

2. Page 1608, line 19-21: Please provide an explanation why change the visible and near infrared albedos for thick ice and cold snow to small values.

Agree. The albedos for sea ice and cold snow were used as tuning parameters during model control simulation.

“The visible and near infrared albedos for thick ice and cold snow are set to 0.77, 0.35, 0.96 and 0.69 respectively, a litter smaller than the standard CICE

configuration.”

Revised to:

“The visible and near infrared albedos for thick ice and cold snow are set to 0.77, 0.35, 0.96 and 0.69 respectively, slightly smaller than the standard CICE configuration, as they are used as tuning parameters during model control integration.”

3. Page 1609, line 20: Is one coupler utilized in the ESM for all the component? Or difference components are coupled through difference coupling codes?

Only one coupler utilized in the BNU-ESM for all components, it’s based on the coupler in CCSM3.5. We will do the following revisions to make it clear:

“The coupling framework of BNU-ESM is largely based on an interim version of NCAR CCSM4, denoted CCSM3.5, with changes on grid mapping interpolation to allow for the identical tripolar grids used in both ocean and sea ice components.”

Revised to:

“The coupling framework of BNU-ESM is largely based on the coupler in NCAR CCSM3.5 (an interim version of NCAR CCSM4), with changes on grid mapping interpolation to allow for the identical tripolar grids used in both ocean and sea ice components. The time evolution of the whole model and communication between various component models are all synchronized and controlled by the coupler in the BNU-ESM.”

4. Page 1610, line 21: Is the pre-industrial run of BNU-ESM an atmospheric only simulation? Should indicate this in the text.

The pre-industrial run of BNU-ESM for providing physical quantities to off-line carbon cycle integrations was done with the whole coupled model but turning carbon cycles off. We would do the following revisions to indicate it clearly:

“In these off-line integrations of the first step spin-up, surface physical quantities such as winds, temperature, precipitation, moisture, and radiation flux are taken as the climatology of a pre-industrial run of BNU-ESM with carbon cycles turned off.”

Revised to:

“In these off-line integrations of the first step spin-up, surface physical quantities

such as winds, temperature, precipitation, moisture, and radiation flux are taken as the climatology of a pre-industrial run of the fully-coupled BNU-ESM with carbon cycles turned off.”

5. Page 1611, line 12: "is" is missing in the sentence (Note the there is no land cover change....)

Agree and thanks.

“Note that there no land cover change related to (anthropogenic) land use...”

Revised to:

“Note that there is no land cover change related to (anthropogenic) land use...”

6. Page 1611, line 24: it’s worth mentioned that the positive temperature bias consistent with low cloud fraction, precipitation and excessive net shortwave at TOA is documented in Ma et al. (2014), Journal of Climate. The positive temperature is even larger over the central US during northern summer.

Agree and thanks for this suggestion. Updated Fig. 3 in minor comment 8, Fig. 4 in minor comment 9, and newly added Fig. R6, Fig. R7 in minor comment 10 confirm the above conclusion in Ma et al. (2014), such as positive temperature biases and less cloud fraction over central USA, west-south Europe. On the other hand, the temperature biases over continents are more consistent with TOA shortwave cloud forcing (SWCF) biases (Fig. 3b and Fig R6b), such as negative temperature biases over western USA, South Africa and South America are likely linked to negative SWCF biases.

7. Figure 1 & 2: include shading to indicate the interannual variability (standard deviation).

Agree and done. Please check the following improved figures:

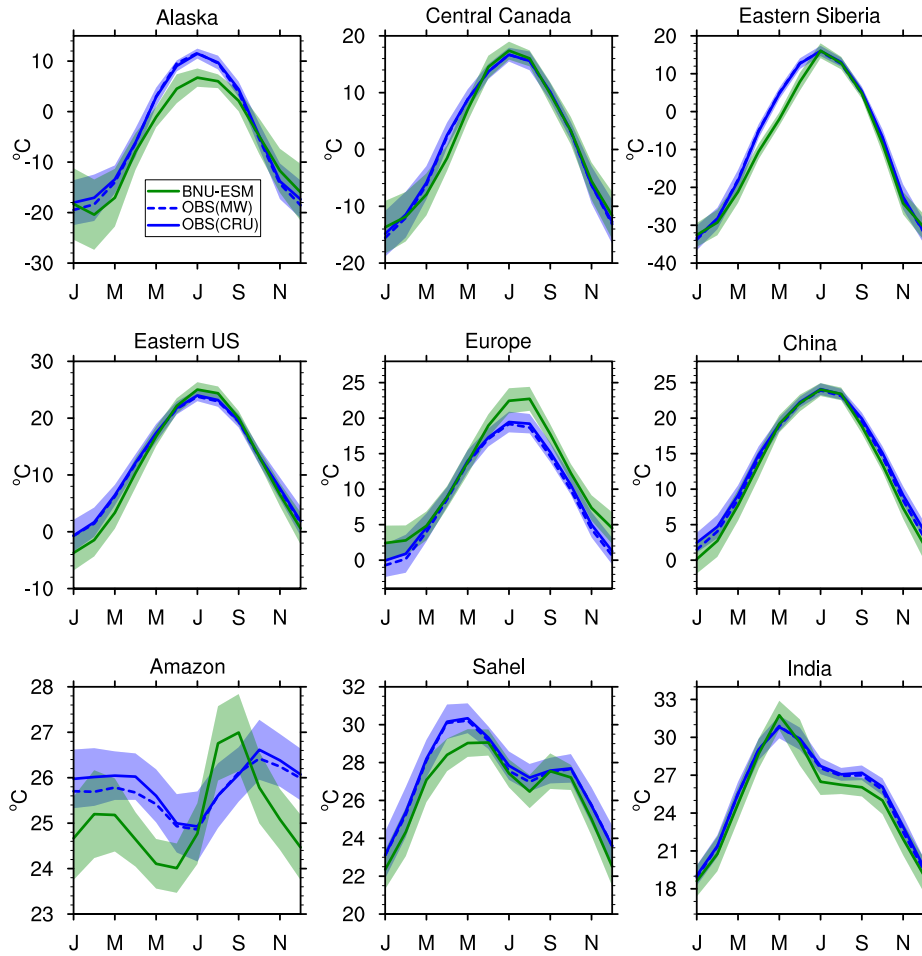


Figure 1. Climatological annual cycle of 2-m air temperature for selected regions for BNU-ESM and two observational estimates for the period 1976-2005. Color shading indicates interannual variability (standard deviation). MW denotes version 2.01, $0.5^{\circ} \times 0.5^{\circ}$ monthly time series from Matsuura and Willmott (2009a). CRU is the Climatic Research Unit $0.5^{\circ} \times 0.5^{\circ}$ TS 3.1 dataset (Harris et al., 2013). Regions are defined as follows: Alaska (56° - 75° N, 167° - 141° W), Central Canada (46° - 61° N, 123° - 97° W), Eastern Siberia (51° - 66° N, 112° - 138° E), eastern United States (27° - 47° N, 92° - 72° W), Europe (37° - 57° N, 0° - 32° E), China (18° - 42° N, 100° - 125° E), Amazon (14° S- 5° N, 74° - 53° W), Sahel (4° - 19° N, 0° - 32° E), and India (4° - 28° N, 68° - 94° E).

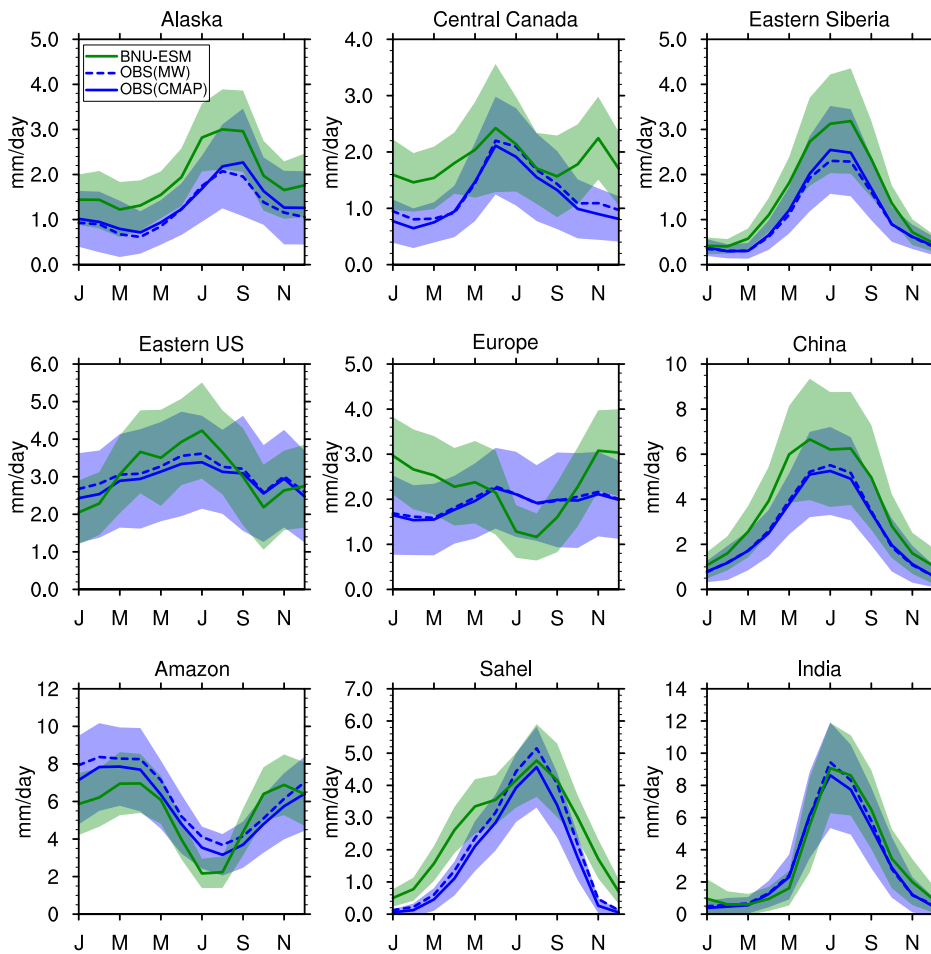


Figure 2. As for Figure 1, but for precipitation for the period 1979-2005. Color shading indicates interannual variability (standard deviation). CMAP comes from the Climate Prediction Center (CPC) Merged Analysis of Precipitation 1979-2009 “standard” (no reanalysis data) monthly time series at $2.5^{\circ} \times 2.5^{\circ}$ (Xie and Arkin, 1997). MW is version 2.01, $0.5^{\circ} \times 0.5^{\circ}$ monthly time series from Matsuura and Willmott (2009b) for the years 1979-2005.

8. Figure 3: statistical test (e.g., T-test) is necessary to show the significance of the SST biases. Also, it should be biases rather than differences.

Agree and Done. The climatological mean field from observations was also added according to review#1 minor comment 2.

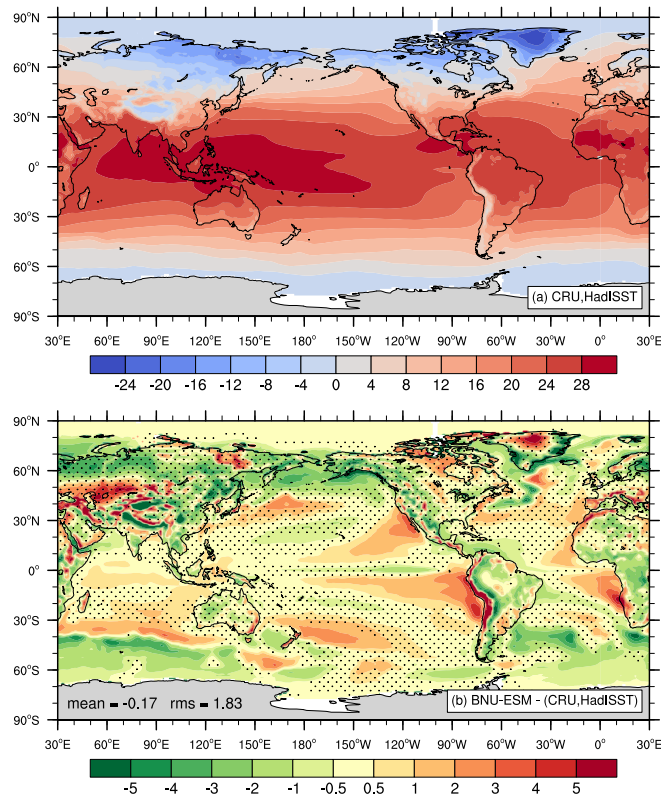


Figure 3. Climatological mean surface temperature from the $0.5^\circ \times 0.5^\circ$ CRU TS 3.1 (Harris et al., 2013) and $1^\circ \times 1^\circ$ HadISST (Rayner et al., 2003) observations (a) for the period 1976-2005. Annual mean surface temperature bias ($^\circ\text{C}$) of BNU-ESM relative to the CRU TS 3.1 and HadISST data sets for the period 1976-2005 (b). All data sets are regridded to $1^\circ \times 1^\circ$ resolution. Dotted area indicates non-significant regions at the 95% confidence level.

9. Figure 4: same as comment 8. Also, the GPCP also have values over land, why not also show the biases over land?

Agree and Done. The climatological mean field from observations was also added according to review#1 minor comment 2.

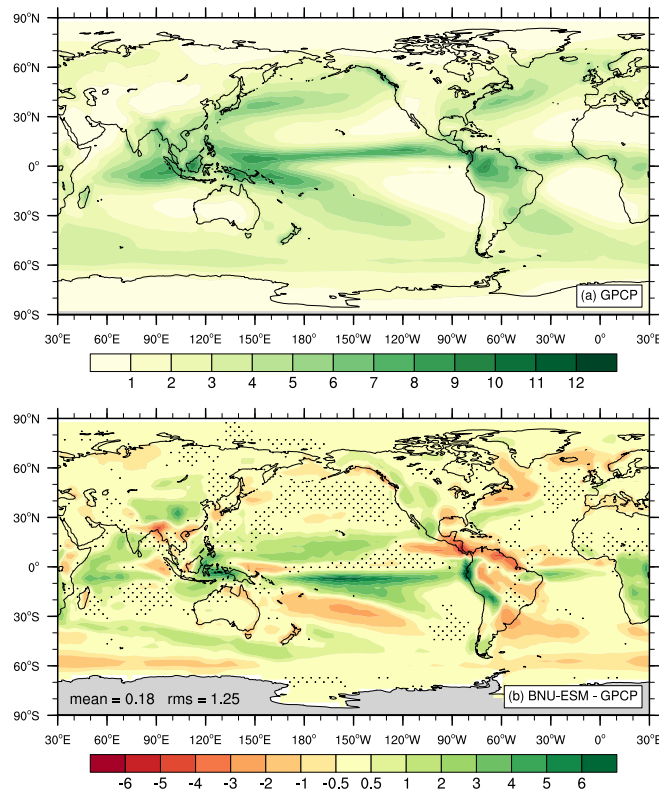


Figure 4. Climatological mean precipitation from the GPCP observations (a) and annual mean precipitation bias (mm/day) of BNU-ESM relative to the GPCP climatology for the period 1979-2005. Dotted area indicates non-significant regions at the 95% confidence level.

10. Page 1613, line 2: So, the BNU-ESM model actual produce too much cloud fraction? How about the total water path? A figure is probably not necessary but a sentence or two would be better to describe the performance of simulated cloud liquid and ice over Southern Ocean. This is interesting since most of the climate models produce too few clouds and too much net shortwave radiation at the surface.

Sorry we were wrong on this conclusion. BNU-ESM model actually produces less cloud fraction. In South Atlantic and South Indian Oceans, the shortwave cloud radiation effect has a small positive bias in the cold band between 40°S and 50°S. We will delete this sentence (Page 1613, line2) from the final revised paper. The following figures on total cloud fraction bias (Fig R6) and shortwave cloud radiation effect (Fig. R7) can prove it.

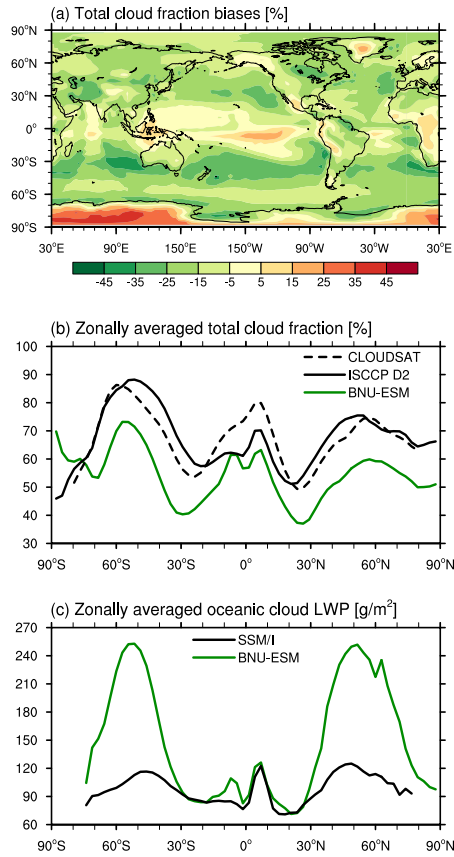


Figure R6. (a) Total cloud fraction bias relative to ISCCP D2 retrievals (Rossow and Schiffer, 1999; Rossow and Dueñas, 2004). (b) Zonally averaged total cloud fraction compared to ISCCP D2 retrievals and CLOUDSAT retrievals (L'Ecuyer et al., 2008.) (c) Zonally averaged total liquid water path (LWP) compared to SSM/I retrievals (Wentz, 2000, 2013) over oceans.

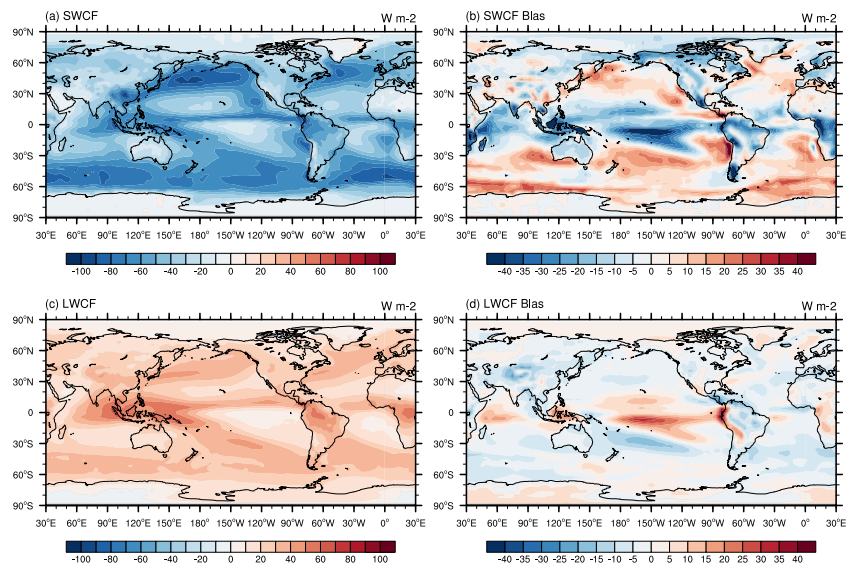


Figure R7. Global map of shortwave cloud forcing (SWCF) and longwave cloud forcing (LWCF): (a) observed CERES-EBAF, (b) BNU-ESM SWCF bias relative to CERES-EBAF, (c) observed CERES-EBAF, (d) BNU-ESM LWCF bias relative to CERES-EBAF.

11. Page 1613, line 19: references?

Thanks. The following references will be added:

Liu, L., Yu, W., Li, T.: Dynamic and Thermodynamic Air–Sea Coupling Associated with the Indian Ocean Dipole Diagnosed from 23 WCRP CMIP3 Models. *J. Climate*, 24, 4941–4958. doi: <http://dx.doi.org/10.1175/2011JCLI4041.1>, 2011.

Cai, W., and Cowan, T.: Why is the amplitude of the Indian Ocean Dipole overly large in CMIP3 and CMIP5 climate models?, *Geophys. Res. Lett.*, 40, 1200–1205, doi:10.1002/grl.50208, 2013.

12. Figure 5a: include the shading for the standard deviations of the monthly mean SSTs to indicate the interannual variability.

Agree and done.

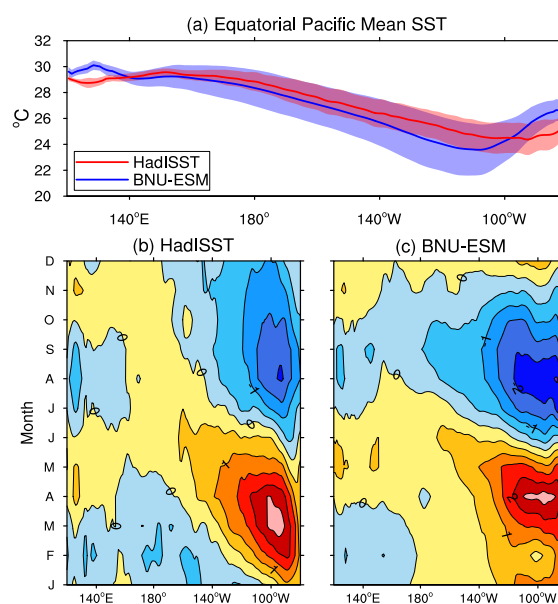


Figure 5. Mean SST (°C) along the equator in the Pacific Ocean (a), color shading indicates interannual variability (standard deviation). Annual cycle of SST anomalies for

the period of 1976-2005 from HadISST (b) and the BNU-ESM *historical* run (c).

13. Page 1615, line 9: delete "much" from "The much too extensive...".

Agree and thanks.

"The much too extensive sea ice simulated in both hemispheres is consistent with the cold SST bias found in corresponding areas (Fig. 3)."

Revised to:

"The too extensive sea ice simulated in both hemispheres is consistent with the cold SST bias found in corresponding areas (Fig. 3)."

14. Page 1615, line 12: Although the reason for the long heat transport may be true, another observations/reanalysis rather than NCEP reanalysis should be used for comparison.

Agree. We also compared the surface wind stress with ERA-Interim reanalysis.

"One notable bias is that the annual averaged zonal wind stress from about 35°S to 55°S latitudes over ocean is 42.8% anomalously stronger compared with NCEP reanalysis products..."

Revised to:

"One notable bias is that the annual average zonal wind stress from about 35°S to 55°S latitudes over ocean is 23.2% stronger compared with ERA-Interim reanalysis and 42.8% stronger compared with NCEP reanalysis..."

15. Figure 11, the power spectra are too noisy. Some smoothing function for the power spectra to better show the interannual band is necessary. Only three year peak is evident. The 7 year is not obvious in the current plot.

Agree. To clearly indicate the 3-7 years range from observations, we added two vertical dashed lines at 3yr and 7yr and one horizontal line in the figure.

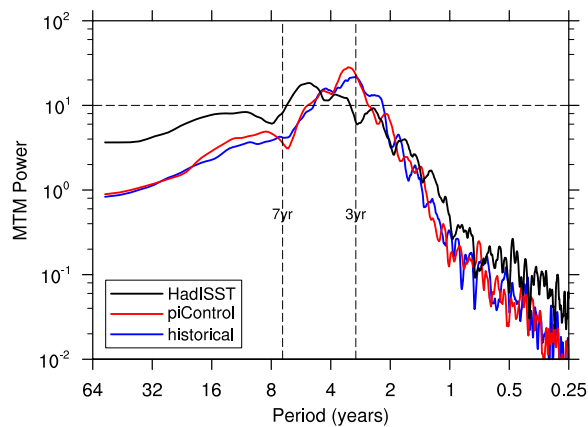


Figure 11. Power spectra of the Niño-3.4 index (the SST anomalies of Figure 10 normalized with the standard deviation) using the multitaper method (Ghil et al., 2002) with resolution $p=4$ and number of tapers $t=7$.

References

Anav, A, Friedlingstein, P., Kidston, M., Bopp, L., Ciais, P., Cox, P., Jones, C., Jung, M., Myneni, R., and Zhu, Z.: Evaluating the Land and Ocean Components of the Global Carbon Cycle in the CMIP5 Earth System Models, *J. Climate*, 26, 6801–6843, doi: <http://dx.doi.org/10.1175/JCLI-D-12-00417.1>, 2013.

Aumann, H. H.; Chahine, M. T.; Gautier, C.; Goldberg, M. D.; Kalnay, E.; McMillin, L. M.; Revercomb, H.; Rosenkranz, P. W.; Smith, W. L.; Staelin, D. H.; Strow, L. L.; Susskind, J.: AIRS/AMSU/HSB on the aqua mission: Design, science objectives, data products, and processing systems, *IEEE Trans. Geosci. Remote Sens.*, 41(2), 253–264, doi:10.1109/tgrs.2002.808356, 2003.

Barkstrom, B. R.: The earth radiation budget experiment, *Bull. Am. Meteorol. Soc.*, 65, 1170–1185, 1984.

Beer, C., Reichstein, M., Tomelleri, E., Ciais, P., Jung, M., Carvalhais, N., Rödenbeck, C., Arain, M. A., Baldocchi, D., Bonan, G. B., Bondeau, A., Cescatti, A., Lasslop, G., Lindroth, A., Lomas, M., Luysaert, S., Margolis, H., Oleson, K. W., Rouspard, O., Veenendaal, E., Viovy, N., Williams, C., Woodward, F. I., and Papale, D.: Terrestrial gross carbon dioxide uptake:

Global distribution and covariation with climate, *Science*, 329, 834–838, 2010.

Chahine, M. T., and Coauthors: AIRS: Improving weather forecasting and providing new data on greenhouse gases, *Bull. Amer. Meteor. Soc.*, 87(7), 911–926, doi:10.1175/bams-87-7-911, 2006.

Chang, C.-P., Zhang, Y., Li, T.: Interannual and Interdecadal Variations of the East Asian Summer Monsoon and Tropical Pacific SSTs. Part I: Roles of the Subtropical Ridge. *J. Climate*, 13, 4310–4325. doi: [http://dx.doi.org/10.1175/1520-0442\(2000\)013<4310:IAIVOT>2.0.CO;2](http://dx.doi.org/10.1175/1520-0442(2000)013<4310:IAIVOT>2.0.CO;2), 2000.

Ciais, P., Sabine, C., Bala, G., Bopp, L., Brovkin, V., Canadell, J., Chhabra, A., DeFries, R., Galloway, J., Heimann, M., Jones, C., Quéré, C. L., Myneni, R. B., Piao, S., and Thornton, P.: Carbon and Other Biogeochemical Cycles. In: *Climate Change 2013: The Physical Science Basis. Contribution of Working Group I to the Fifth Assessment Report of the Intergovernmental Panel on Climate Change*, Cambridge University Press, Cambridge, United Kingdom and New York, NY, USA. 2013.

Dee, D. P., Uppala, S. M., Simmons, A. J., Berrisford, P., Poli, P., Kobayashi, S., Andrae, U., Balmaseda, M. A., Balsamo, G., Bauer, P., Bechtold, P., Beljaars, A. C. M., van de Berg, L., Bidlot, J., Bormann, N., Delsol, C., Dragani, R., Fuentes, M., Geer, A. J., Haimberger, L., Healy, S. B., Hersbach, H., Hólm, E. V., Isaksen, I., Kållberg, P., Köhler, M., Matricardi, M., McNally, A. P., Monge-Sanz, B. M., Morcrette, J.-J., Park, B.-K., Peubey, C., de Rosnay, P., Tavolato, C., Thépaut, J.-N. and Vitart, F.: The ERA-Interim reanalysis: configuration and performance of the data assimilation system. *Q.J.R. Meteorol. Soc.*, 137: 553–597. doi: 10.1002/qj.828, 2011.

Ebita, A., Kobayashi, S., Ota, Y., Moriya, M., Kumabe, R., Onogi, K., Harada, Y., Yasui, S., Miyaoka, K., Takahashi, K., Kamahori, H., Kobayashi, C., Endo, H., Soma, M., Oikawa, Y., and Ishimizu, T.: The Japanese 55-year Reanalysis “JRA-55”: An Interim Report, *SOLA*, Vol. 7, 149–152, doi:10.2151/sola.2011-038, 2011.

FAO/IIASA/ISRIC/ISSCAS/JRC, Harmonized World Soil Database (version 1.2). FAO,

Rome, Italy and IIASA, Laxenburg, Austria. 2012.

Gleckler, P. J., Taylor, K. E., and Doutriaux, C.: Performance metrics for climate models, *J. Geophys. Res.*, 113, D06104, doi:10.1029/2007JD008972, 2008.

Gruber, N., Friedlingstein, P., Field, C. B., Valentini, R., Heimann, M., Richey, J. E., Lankao, P. R., Schulze, E.-D., and Chen, C.-T. A.: The vulnerability of the carbon cycle in the 21st century: An assessment of carbon-climate-human interactions. In: *The Global Carbon Cycle: Integrating Humans, Climate, and the Natural World* (eds Field CB, Raupach MR), Island Press, Washington, Covelo, London, 2004.

Hung, M.-P., Lin, J.-L., Wang, W., Kim, D., Shinoda, T., Weaver, S. J.: MJO and Convectively Coupled Equatorial Waves Simulated by CMIP5 Climate Models. *J. Climate*, **26**, 6185–6214. doi: <http://dx.doi.org/10.1175/JCLI-D-12-00541.1>, 2013.

IGBP-DIS: Global Soil Data Task Group. Global Gridded Surfaces of Selected Soil Characteristics. [Global Gridded Surfaces of Selected Soil Characteristics (International Geosphere-Biosphere Programme - Data and Information System)]. Data set. Available online at <http://daac.ornl.gov/SOILS/guides/igbp-surfaces.html> (last access: May 2014) from Oak Ridge National Laboratory Distributed Active Archive Center, Oak Ridge, Tennessee, U.S.A. doi:10.3334/ORNLDAAC/569. 2000.

Ito, A.: A historical meta-analysis of global terrestrial net primary productivity: are estimates converging?. *Global Change Biology*, 17, 3161–3175. doi: 10.1111/j.1365-2486.2011.02450.x, 2011.

Josey, S. A., Kent, E. C., and Taylor, P. K.: New insights into the ocean heat budget closure problem from analysis of the SOC air-sea flux climatology, *J. Climate*, 12, 2856–2880, 1999.

Jung, M., Reichstein, M., Margolis, H. A., Cescatti, A., Richardson, A. D., Arain, M. A., Arneth, A., Bernhofer, C., Bonal, D., Chen, J., Gianelle, D., Gobron, N., Kiely, G., Kutsch, W., Lasslop, G., Law, B. E., Lindroth, A., Merbold, L., Montagnani, L., Moors, E. J., Papale, D.,

Sottocornola, M., Vaccari, F., and Williams, C.: Global patterns of land-atmosphere fluxes of carbon dioxide, latent heat, and sensible heat derived from eddy covariance, satellite, and meteorological observations, *J. Geophys. Res.*, 116, G00J07, doi:10.1029/2010JG001566, 2011.

Jobbágy, E. G. and Jackson, R. B.: The vertical distribution of soil organic carbon and its relation to climate and vegetation, *Ecol. Appl.*, 10, 423–436. [http://dx.doi.org/10.1890/1051-0761\(2000\)010\[0423:TVDOSO\]2.0.CO;2](http://dx.doi.org/10.1890/1051-0761(2000)010[0423:TVDOSO]2.0.CO;2). 2000.

L'Ecuyer, T. S., Wood, N. B., Haladay, T., Stephens, G. L., and Stackhouse Jr., P. W.: Impact of clouds on atmospheric heating based on the R04 CloudSat fluxes and heating rates data set, *J. Geophys. Res.*, 113, D00A15, doi:10.1029/2008JD009951, 2008.

Li, H., Dai, A., Zhou, T., and Lu, J.: Responses of East Asian summer monsoon to historical SST and atmospheric forcing during 1950–2000, *Climate Dynamics*, Volume 34, Issue 4, pp 501-514, 2010.

Lloyd, J. and Taylor, J. A.: On the temperature dependence of soil respiration, *Funct. Ecol.*, 8, 315–323, 1994.

Loeb, N. G., Wielicki, B. A., Doelling, D. R., Smith, G. L., Keyes, D. F., Kato, S., Manalo-Smith, N., and Wong, T.: Toward optimal closure of the earth's top-of-atmosphere radiation budget. *J. Climate*, 22, 748–766, 2009.

Reynolds, R. W., Rayner, N. A., Smith, T. M., Stokes, D. C., and Wang, W.: An improved in situ and satellite SST analysis for climate, *J. Climate*, 15, 1609-1625, 2002.

Rienecker, M. M., and Coauthors: MERRA: NASA's Modern-Era Retrospective Analysis for Research and Applications, *J. Climate*, 24(14), 3624–3648, doi:10.1175/jcli-d-11-00015.1, 2011.

Rossow, W. B., Dueñas, E. N.: The International Satellite Cloud Climatology Project

(ISCCP) Web Site: An Online Resource for Research. *Bull. Amer. Meteor. Soc.*, 85, 167–172. doi: <http://dx.doi.org/10.1175/BAMS-85-2-167>, 2004.

Rossow, W. B., and Schiffer, R. A.: Advances in understanding clouds from ISCCP, *Bull. Am. Meteorol. Soc.*, 80, 2261–2287, 1999.

Sabine, C. L., Feely, R. A., Gruber, N., Key, R. M., Lee, K., Bullister, J. L., Wanninkhof, R., Wong, C. S., Wallace, D. W. R., Tilbrook, B., Millero, F. J., Peng, T.-H., Kozyr, A., Ono, T., and Rios, A. F.: The oceanic sink for anthropogenic CO₂. *Science*, 305, 367–371, 2004.

Schimel, D. S., House, J. I., Hibbard, K. A., Bousquet, P., Ciais, P., Peylin, P., Braswell, B. H., Apps, M. J., Baker, D., Bondeau, A., Canadell, J., Churkina, G., Cramer, W., Denning, A. S., Field, C. B., Friedlingstein, P., Goodale, C., Heimann, M., Houghton, P. A., Melillo, J. M., Moore, B., III, Murdiyarso, D., Noble, I., Pacala, S. W., Prentice, I. C., Raupach, M. R., Rayner, P. J., Scholes, R. J., Steffen, W. L., and Wirth, C.: Recent patterns and mechanisms of carbon exchange by terrestrial ecosystems. *Nature*, 414, 169–172, 2001.

Simpson, J. J., and Coauthors: The NVAP global water vapor dataset: Independent cross-comparison and multiyear variability, *Remote Sens. Environ.*, 76, 112–129, 2001.

Takahashi, T., Sutherland, S. C., Wanninkhof, R., Sweeney, C., Feely, R. A., Chipman, D. W., Hales, B., Friederich, G., Chavez, F., Sabine, C., Watson, A., Bakker, D. C. E., Schuster, U., Metzl, N., Yoshikawa-Inoue, H., Ishii, M., Midorikawa, T., Nojiri, Y., Körtzinger, A., Steinhoff, T., Hoppema, M., Olafsson, J., Arnarson, T. S., Tilbrook, B., Johannessen, T., Olsen, A., Bellerby, R., Wong, C. S., Delille, B., Bates, N. R., de Baar, H. J. W.: Climatological mean and decadal change in surface ocean pCO₂, and net sea–air CO₂ flux over the global oceans, *Deep Sea Research Part II: Topical Studies in Oceanography*, Volume 56, Issues 8–10, April 2009, Pages 554–577, ISSN 0967-0645, <http://dx.doi.org/10.1016/j.dsr2.2008.12.009>.

Tarnocai, C., Canadell, J. G., Schuur, E. A. G., Kuhry, P., Mazhitova, G., and Zimov, S.: Soil organic carbon pools in the northern circumpolar permafrost region, *Global Biogeochem. Cy.*, 23, GB2023, doi:10.1029/2008GB003327, 2009.

Todd-Brown, K. E. O., Randerson, J. T., Post, W. M., Hoffman, F. M., Tarnocai, C., Schuur, E. A. G., and Allison, S. D.: Causes of variation in soil carbon simulations from CMIP5 Earth system models and comparison with observations, *Biogeosciences*, 10, 1717–1736, doi:10.5194/bg-10-1717-2013, 2013.

Tarnocai, C., Canadell, J. G., Schuur, E. A. G., Kuhry, P., Mazhitova, G., and Zimov, S.: Soil organic carbon pools in the northern circumpolar permafrost region, *Global Biogeochem. Cycles*, 23, GB2023, doi:10.1029/2008GB003327, 2009.

Taylor, K. E.: Summarizing multiple aspects of model performance in a single diagram, *J. Geophys. Res.*, 106, 7183–7192, 2001.

Taylor, P. K. (Ed.): Final report of the Joint WCRP/SCOR Working Group on Air-Sea Fluxes: Intercomparison and validation of ocean-atmosphere energy flux fields. WCRP-112, 2000. Available at http://eprints.soton.ac.uk/69522/1/wgasf_final_rep.pdf (last access: May 2014).

Tian, B., Fetzer, E. J., Kahn, B. H., Teixeira, J., Manning, E., and Hearty, T.: Evaluating CMIP5 Models using AIRS Tropospheric Air Temperature and Specific Humidity Climatology, *J. Geophys. Res. Atmos.*, 118, 114–134, doi:10.1029/2012JD018607, 2013.

Wang, X. J., Behrenfeld, M., Le Borgne, R., Murtugudde, R., and Boss, E.: Regulation of phytoplankton carbon to chlorophyll ratio by light, nutrients and temperature in the Equatorial Pacific Ocean: a basin-scale model, *Biogeosciences*, 6, 391-404, 2009a.

Wang, X. J., Le Borgne, R., and Murtugudde, R.: Nitrogen uptake and regeneration pathways in the equatorial Pacific: a basin scale modeling study, *Biogeosciences*, 6, 2647-2660, 2009b.

Wang, X. J., Le Borgne, R., Murtugudde, R., Busalacchi, A. J., and Behrenfeld, M.: Spatial and temporal variations in dissolved and particulate organic nitrogen in the equatorial Pacific: biological and physical influences, *Biogeosciences*, 5, 1705-1721, 2008.

Welp, L. R., Keeling, R. F., Meijer, H. A. J., Bollenbacher, A. F., Piper, S. C., Yoshimura, K., Francey, R. J., Allison, C. E., and Wahlen, M.: Interannual variability in the oxygen isotopes of atmospheric CO₂ driven by El Niño, *Nature*, 477, 579–582, 2011.

Wentz, F. J.: "SSM/I Version-7 Calibration Report", Remote Sensing Systems, Santa Rosa, CA. 2013. Available at http://www.remss.com/papers/tech_reports/2012_Wentz_011012_Version-7_SSMI_Calibration.pdf (last access: May 2014).

Wentz, F. J.: A well-calibrated ocean algorithm for SSM/I, *J. Geophys. Res.*, 102, 8703–8718, 2000.

Wheeler, M. C., and Kiladis, G. N.: Convectively coupled equatorial waves: Analysis of clouds and temperature in the wavenumber–frequency domain. *J. Atmos. Sci.*, 56, 374–399, 1999.

Wielicki, B. A., and Coauthors: Clouds and the Earth's Radiant Energy System (CERES): An Earth observing system experiment, *Bull. Am. Meteorol. Soc.*, 77, doi:10.1175/1520-0477, 853–868, 1996.

Yuan, H., Dickinson, R. E., Dai, Y., Shaikh, M. J., Zhou, L., Shangguan, W., Ji, D.: A 3D Canopy Radiative Transfer Model for Global Climate Modeling: Description, Validation, and Application. *J. Climate*, 27, 1168–1192. doi: <http://dx.doi.org/10.1175/JCLI-D-13-00155.1>, 2014.

Zhao, M. S., Heinsch, F. A., Nemani, R. R., and Running, S. W.: Improvements of the MODIS terrestrial gross and net primary production global data set, *Remote Sens. Environ.*, 95, 164–176, doi:10.1016/j.rse.2004.12.011, 2005.